Cell Research (2012) 22:360-371.

www.nature.com/cr

ORIGINAL ARTICLE

Cleavage of serum response factor mediated by enteroviral protease 2A contributes to impaired cardiac function

Jerry Wong[1], Jingchun Zhang[1], Bobby Yanagawa[1], Zongshu Luo[1], Xiangsheng Yang[2], Jiang Chang[2], Bruce McManus[1], Honglin Luo[1]

[1]James Hogg iCAPTURE Centre, Providence Heart + Lung Institute, St Paul's Hospital and Department of Pathology and Laboratory Medicine, University of British Columbia, 1081 Burrard Street, Vancouver, BC V6Z 1Y, Canada; [2]Center for Molecular Development and Disease, Institute of Biosciences and Technology, Texas A&M Health Science Center, Houston, TX 77030, USA

Enteroviral infection can lead to dilated cardiomyopathy (DCM), which is a major cause of cardiovascular mortality worldwide. However, the pathogenetic mechanisms have not been fully elucidated. Serum response factor (SRF) is a cardiac-enriched transcription regulator controlling the expression of a variety of target genes, including those involved in the contractile apparatus and immediate early response, as well as microRNAs that silence the expression of cardiac regulatory factors. Knockout of SRF in the heart results in downregulation of cardiac contractile gene expression and development of DCM. The goal of this study is to understand the role of SRF in enterovirus-induced cardiac dysfunction and progression to DCM. Here we report that SRF is cleaved following enteroviral infection of mouse heart and cultured cardiomyocytes. This cleavage is accompanied by impaired cardiac function and downregulation of cardiac-specific contractile and regulatory genes. Further investigation by antibody epitope mapping and site-directed mutagenesis demonstrates that SRF cleavage occurs at the region of its transactivation domain through the action of virus-encoded protease 2A. Moreover, we demonstrate that cleavage of SRF dissociates its transactivation domain from DNA-binding domain, resulting in the disruption of SRF-mediated gene transactivation. In addition to loss of functional SRF, finally we report that the N-terminal fragment of SRF cleavage products can also act as a dominant-negative transcription factor, which likely competes with the native SRF for DNA binding. Our results suggest a mechanism by which virus infection impairs heart function and may offer a new therapeutic strategy to ameliorate myocardial damage and progression to DCM.

Keywords**:** viral cardiomyopathy; enterovirus; coxsackievirus; enteroviral protease 2A; viral myocarditis
Cell Research (2012) **22**:360-371. doi:10.1038/cr.2011.114; published online 19 July 2011

Introduction

Enteroviruses, such as coxsackievirus B3 (CVB3), are among the most prevalent and well-studied etiological agents associated with viral myocarditis, an inflammatory disease of the myocardium [1, 2]. Viral myocarditis can lead to reduced cardiac function and the progression to dilated cardiomyopathy (DCM), which is an important cause of cardiovascular mortality worldwide, particularly in children [1, 2]. However, the mechanism underlying progression from acute infection to development of a dilated cardiac phenotype is not fully understood.

Enteroviral-encoded proteases have been recognized as important pathogenic factors contributing to the development of DCM. Enterovirus encodes viral proteases 2A and 3C, which cleave multiple host proteins essential for the maintenance of cellular architecture, protein translation, transcription, and cell signaling in addition to the processing of viral polyprotein [1]. Transgenic mice with cardiac-restricted expression of protease 2A develop severe cardiac dysfunction and DCM [3]. Disruption of the dystrophin-glycoprotein complex through dystrophin cleavage has been proposed as one important mechanism in the progression of DCM [4]. However, dystrophin-

Correspondence: Honglin Luo
Tel: +1-604-682-2344 ext. 62847; Fax: +1-604-806-9274
E-mail: honglin.luo@hli.ubc.ca
Received 25 January 2011; revised 12 April 2011; accepted 4 May 2011; published online 19 July 2011

null mice do not develop equally severe cardiomyopathy [5, 6] as observed in 2A transgenic mice, suggesting that other molecular targets may also exist and contribute to the viral pathogenesis.

Serum response factor (SRF) is a member of the MADS (MCM1, Agamous, Deficiens, and SRF) box superfamily of transcription factors. It binds to serum response element (SRE, also known as CArG box (CC(A/T)$_6$GG)) and is associated with the regulation of a variety of target genes, including immediate early, contractile, and microRNA (miRNA) genes [7-9]. A genome-wide search for SRF targets has identified approximately 1 200 genes, which contain single or more copies of this consensus SRE sequence in their promoter regions (termed CArGome) [10]. More than 250 of these genes have been validated [10].

SRF is highly expressed in cardiac muscle and plays a central role in cardiac development and function by regulating genes for cardiac contractile and regulatory proteins as well as silencer miRNAs [11-14]. Recent studies have identified several miRNAs as targets of SRF in the heart, which include miR-486 [15], miR-133a [11, 14], and miR-1 [16]. Expression of these miRNAs controls heart development and function by repressing the expression of cardiac regulatory proteins. In mice, cardiac-specific knockout of SRF gene is embryonic lethal due to defects in cardiogenesis [12, 14, 17]. Using the Cre/LoxP system, disruption of SRF gene in adult heart leads to impaired cardiac function, subsequently progressing to DCM [18]. Furthermore, we have previously reported that cleavage of SRF by caspase-3 plays an important role in the progression of human heart failure [19].

The objective of the present study is to elucidate a potentially novel molecular mechanism involved in the impaired heart function and development of DCM. Here we demonstrate that SRF is cleaved during CVB3 infection through the action of viral protease 2A. Such cleavage leads to the dissociation of the DNA-binding domain of SRF from its transactivation domain, resulting in the disruption of SRF-mediated gene transactivation and the generation of a dominant-negative transcription factor, which competes with the native SRF for DNA binding. Our results suggest an important mechanism by which CVB3 damages cardiac function and leads to subsequent DCM.

Results

Cardiac function and cardiac gene expression following CVB3 infection

The mouse model of myocarditis has been well characterized and commonly used to study target organ injury during CVB3 infection [20, 21]. Two-dimensional echocardiography was performed to assess functional alterations in CVB3-infected mouse hearts. As shown in Figure 1A, virus-infected mice displayed cardiac dysfunction, evidenced by a significant reduction in left ventricular posterior wall (LVPW) thickening and ejection fraction.

Heart failure has been associated with the reduction of a broad range of cardiac-specific genes [22-24]. To determine the cardiac gene expression, we performed microarray analysis of CVB3-infected mouse hearts and real-time RT-PCR examination of CVB3-infected cardiomyocytes. Affymetrix array analyses demonstrated a marked reduction in the expression of several cardiac-specific contractile and regulatory genes (Figure 1B). See Supplementary information, Table S1 for complete list of Affymetrix gene expression data. Quantitative RT-PCR results in Figure 1C also demonstrate downregulation of several cardiac genes, including ANP, β-MHC, GATA-4, MEF-2, and NFAT, in CVB3-infected cardiomyocytes.

Expression levels of SRF following CVB3 infection

As alluded to earlier, SRF is a cardiac-enriched transcription factor, regulating the expression of numerous cardiac-specific genes. To explore whether downregulation of cardiac genes is associated with dysregulation of SRF, we examined the expression levels of SRF during CVB3 infection. Using an antibody against the C-terminus of SRF, we found that CVB3 infection of mouse cardiomyocytes (Figure 2A, top panel) and hearts (Figure 2D) led to marked decreases in the protein expression of SRF (~67 kDa), accompanied by the appearance of ~20 kDa fragments. To validate the results, we used an antibody against the N-terminus of SRF (Novus Biologicals). As shown in Figure 2A bottom panel, an extra band at the molecular weight of ~50 kDa was detected in addition to the full-length SRF following CVB3 infection of mouse cardiomyocytes at 20 h and 24 h. These data suggest that SRF is potentially cleaved during CVB3 infection to generate two cleavage products of approximately 50 and 20 kDa, respectively. We further examined the distribution of SRF following CVB3 infection of mouse cardiomyocytes using anti-C-terminal SRF antibody. Figure 2B showed that SRF was redistributed from the nucleus to the cytoplasm in CVB3-infected cells, whereas it remained in the nucleus of sham-infected cells.

Real-time RT-PCR was also carried out to examine the gene expression of SRF after CVB3 infection of mouse cardiomyocytes. The results in Figure 2C demonstrate unchanged mRNA levels of SRF following CVB3 infection, suggesting that the reduced protein expression of full-length SRF is unlikely due to decreased gene expres-

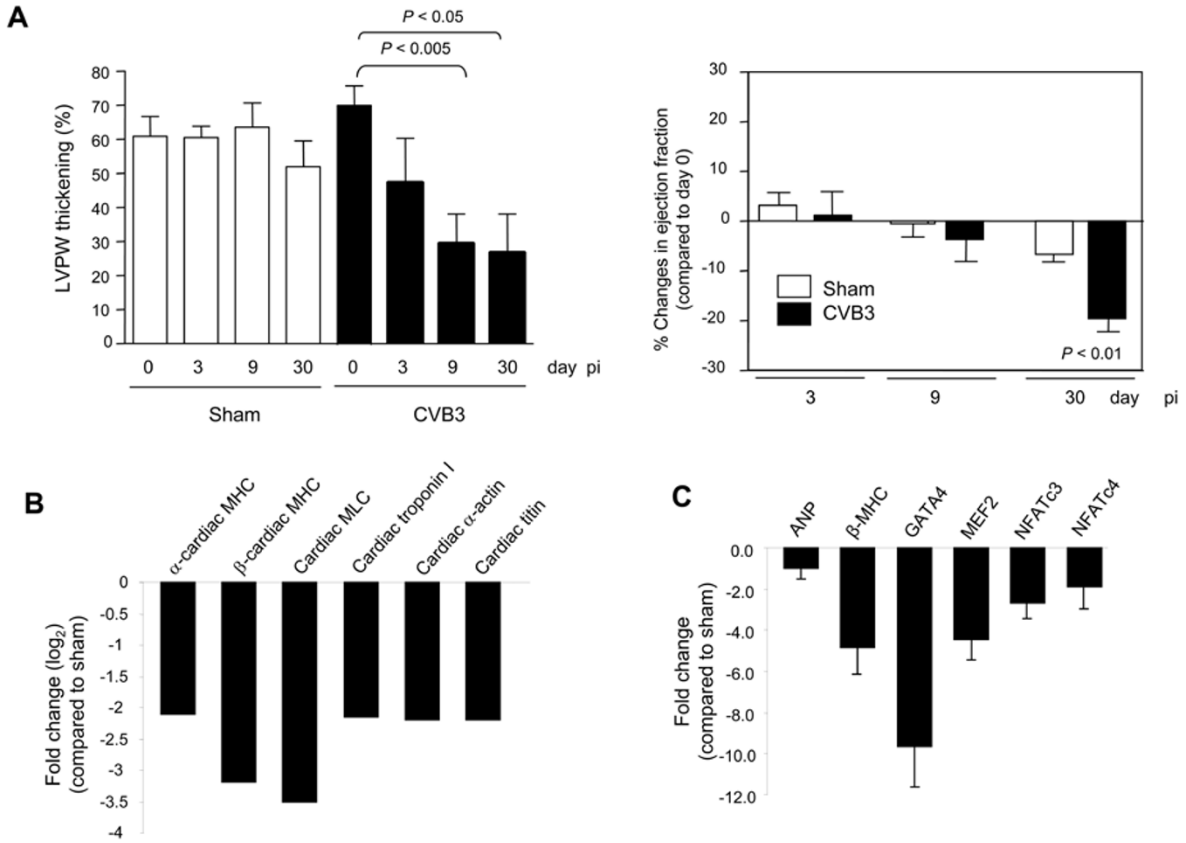

Figure 1 Cardiac function and cardiac gene expression following CVB3 infection. **(A)** Cardiac function following CVB3 infection by echocardiography. At day 0 (before infection), and 3, 9, and 30 days following CVB3 or sham infection of A/J mice, systolic and diastolic parasternal long and short axis measurements were obtained. Left ventricular posterior wall (LVPW) thickening and ejection fraction are presented as percentage changes (mean ± SD, *n* = 4 for each group). pi, post infection. **(B)** CVB3- or sham-infected mouse hearts (*n* = 4 for each group, pooled) at 9 days pi were collected for Affymetrix array analysis. Gene changes in intensity (averages of two replicates of the microarray analysis) were plotted as a ratio of CVB3- to sham-infected hearts for visualization. Only genes that exhibited a 1.8-fold change (log_2) or greater were included. MHC, myosin heavy chain; MLC, myosin light chain. **(C)** Murine HL-1 cardiomyocytes were sham- or CVB3-infected for 24 h. Real-time quantitative RT-PCR was performed to examine the expression of indicated genes. The gene expression was normalized to GAPDH mRNA, and then displayed as fold changes compared to sham infection (mean ± SD, *n* = 3). ANP, atrial natriuretic peptide; MEF2, myocyte enhancer factor 2; NFATc, nuclear factor of activated T cells.

sion, but rather protein cleavage.

Cleavage of SRF following CVB3 infection

To further confirm cleavage of SRF, we utilized a HeLa cell line, a well-characterized model in CVB3 investigations amenable for transfection with plasmids. HeLa cells which express low levels of endogenous SRF were transiently transfected with a 3×FLAG-tagged SRF construct for 48 h followed by CVB3 infection for 7 h. Western blot was performed using anti-FLAG antibody or anti-C-terminal SRF antibody, which showed two cleavage products with molecular weights of ~50 and ~20 kDa, respectively (Figure 3). These results correspond well with our observation on endogenous SRF cleavage shown in Figure 2A.

Caspase-mediated SRF cleavage, which yields a 32-kDa protein fragment, has been reported in both non-cardiac and cardiac cells [19, 25, 26]. To determine whether caspases are involved in CVB3-induced cleavage of SRF, we treated cells with z-VAD-fmk, a general caspase inhibitor. As shown in Figure 4, following CVB3 infection of SRF-transfected cells (lane 6), two cleavage products (~50 and ~40 kDa using anti-N-terminal FLAG antibody and of ~30 and ~20 kDa using anti-C-terminal SRF antibody) were detected. With addition of z-VAD-fmk (lane 7), the levels of the ~40 kDa (upper

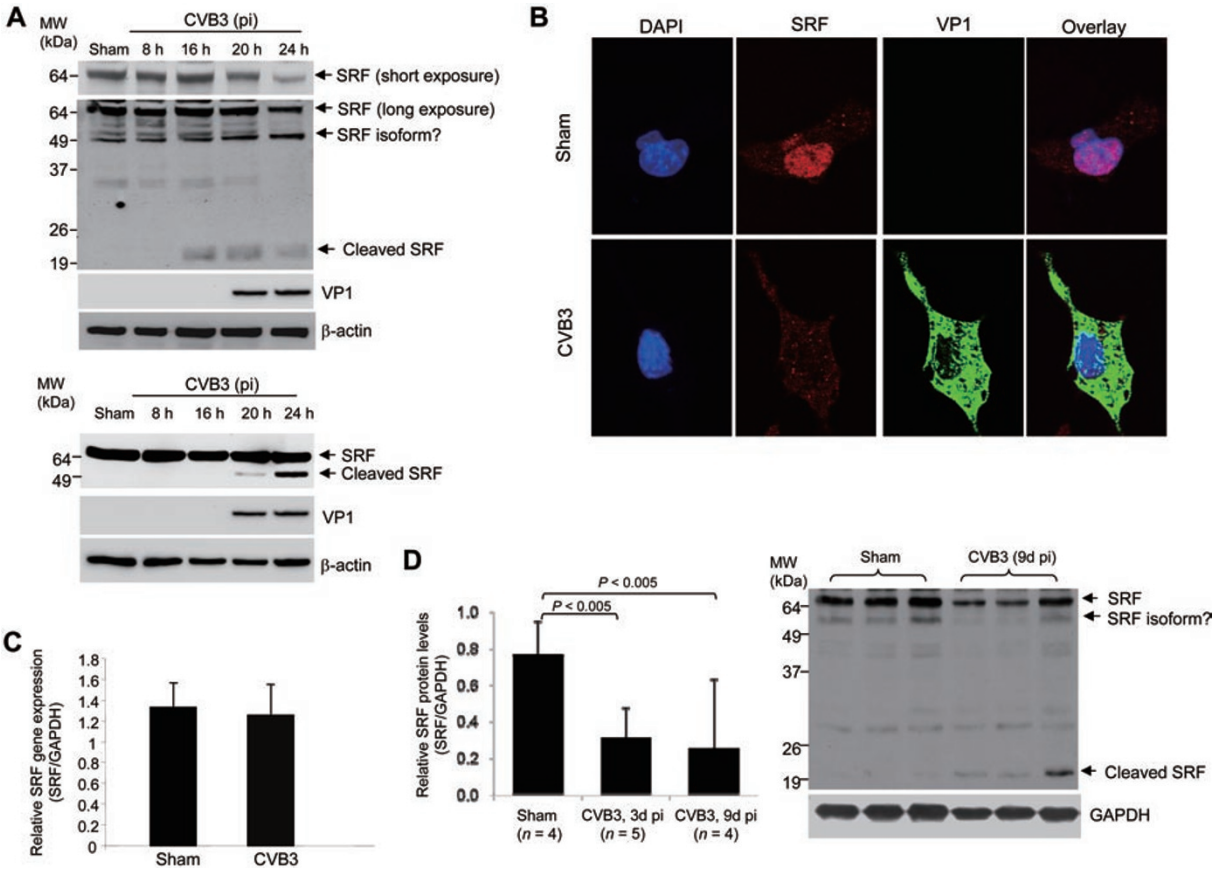

Figure 2 Protein and gene expression of SRF following CVB3 infection. **(A)** Protein expression of SRF following CVB3 infection of murine HL-1 cardiomyocytes. HL-1 cells were either sham infected or infected with CVB3 for various times as indicated. Western blotting was performed to examine protein expression of SRF (top, using anti-C-terminal SRF antibody; bottom, using anti-N-terminal SRF antibody), viral protein VP1 and β-actin (loading control). **(B)** Protein distribution of SRF following CVB3 infection of HL-1 cells. HL-1 cells were infected with CVB3 for 20 h, double-immunocytochemical staining was then performed using anti-C-terminal SRF antibody and anti-VP1 antibody to examine the expression and localization of SRF (red) and viral protein VP1 (green), respectively. The nucleus was counterstained with DAPI (blue). **(C)** Gene expression of SRF after CVB3 infection. RNA samples were extracted from HL-1 cardiomyocytes at 24 h following CVB3 infection. Gene levels of SRF were measured by real-time quantitative RT-PCR and normalized to GAPDH mRNA (mean ± SD, *n* = 3). **(D)** SRF expression in A/J mouse heart following 3 and 9 days of CVB3 infection. Heart extracts were used for western blot analysis of protein expression of SRF (using an anti-C-terminal SRF antibody) and GAPDH (loading control). Left panels, levels of SRF were quantitated by densitometric analysis using NIH ImageJ V1.43, normalized to GAPDH, and presented as mean ± SD. Right panels, representative western blot of SRF expression in mouse heart at 9 days post infection.

panel) and the ~30 kDa (middle panel) fragments were markedly reduced, indicating that they are the cleavage products of SRF by caspases. The appearances of the ~40 kDa (upper panel) and the ~30 kDa (middle panel) bands in SRF-transfected and sham-infected cells (lane 5) are likely due to transfection-induced cytotoxicity. It was noted that inhibition of caspase activation did not prevent the production of the ~50 kDa (lane 7, upper panel) and the ~20 kDa (lane 7, middle panel) fragments, suggesting that these cleavages are independent of caspase activation. Taken together, our results suggest that SRF is cleaved during CVB3 infection by viral protein and caspases at two different sites. Since caspase activation is a late event during viral infection, downregulation of cardiac genes in CVB3-infected mouse heart and cardiomyocytes may be mainly attributable to viral protease-mediated SRF cleavage.

Identification of SRF cleavage site during CVB3 infection

As illustrated in Figure 5A, SRF protein consists of two major domains: the SRE DNA binding and dimeriza-

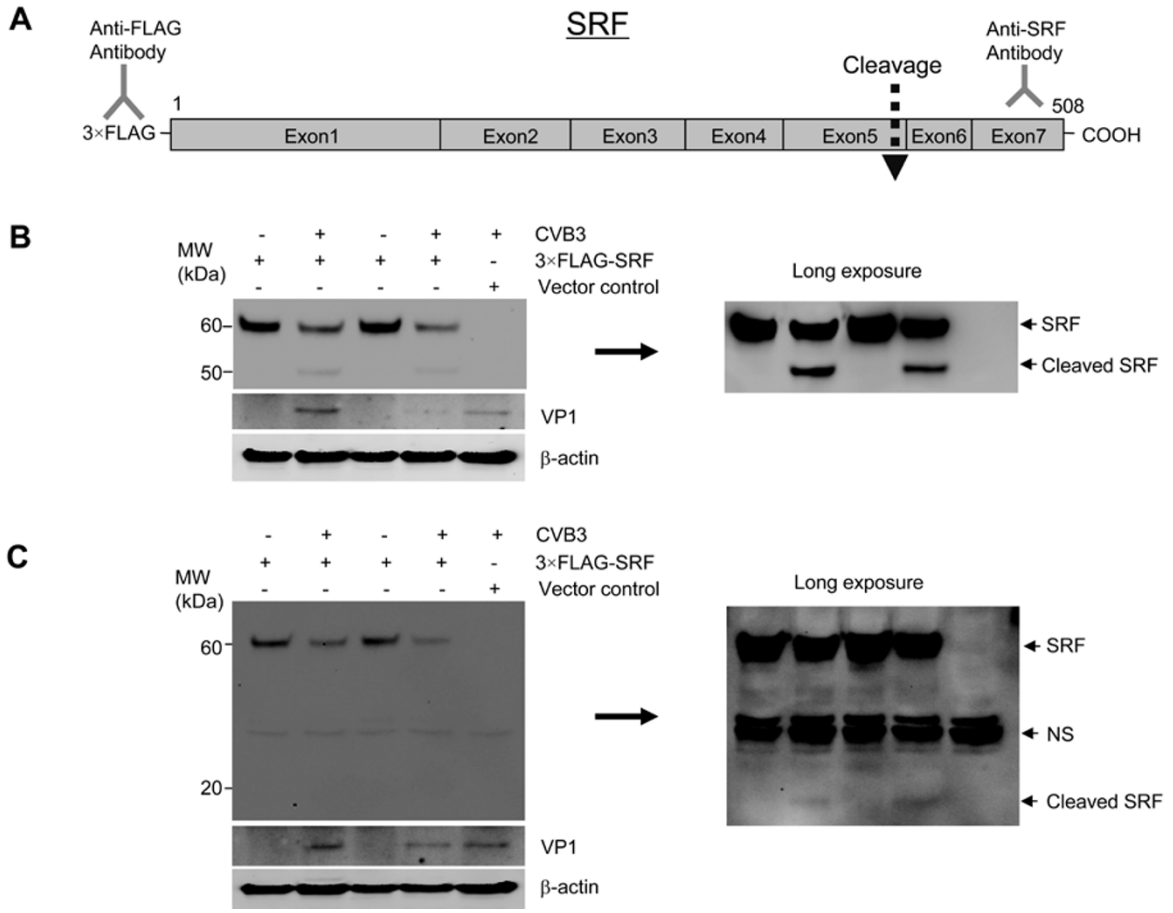

Figure 3 Cleavage of SRF following CVB3 infection. HeLa cells were transiently transfected with a plasmid expressing 3×FLAG-SRF for 48 h, followed by CVB3 infection for 7 h. **(A)** Schematic diagram of the 3×FLAG-SRF construct and western blot detection of SRF with the antibodies described in **B** and **C**. Western blotting was performed to examine protein expression of viral protein VP1, β-actin (loading control), and SRF using an anti-FLAG antibody that recognizes the N-terminus of SRF **(B)** or using an anti-C-terminal SRF antibody **(C)**. NS, nonspecific bands.

tion domain (amino acids 133 to 222) and the transactivation domain (amino acids 339 to 508). Computer prediction algorithm for cleavage sites by enteroviral proteases (NetPicoRNA V1.0 algorithm) revealed potential 2A protease site, which results in two products of ~50 and ~20 kDa (Figure 5A), consistent with the SRF fragments detected in CVB3-infected cells. First, we examined whether SRF can be cleaved by viral protease 2A. Figures 5B and 5C showed that overexpression of 2A resulted in two cleavage products of FLAG-tagged SRF with the molecular weights similar to those observed during CVB3 infection. This study suggests that CVB3 induces SRF cleavage through the action of viral protease 2A.

To confirm the cleavage site predicted by the computer algorithm, we constructed a SRF point mutant, in which the G residue at position 349 was replaced with E (G349E), by site-directed mutagenesis. However, we found that this mutant was still susceptible to cleavage during infection (Figure 6B, upper). To further identify the cleavage site of SRF, we constructed three deletion mutants and a series of point mutation plasmids (data not shown). We found that the G327E mutant was resistant to CVB3-induced cleavage (Figure 6B, lower), suggesting that SRF is cleaved after T326. Although this cleavage site is not predicted by the NetPicoRNA program, amino acid sequence alignments of SRF with other known 2A substrates at the cleavage region revealed a similar cleavage motif (Figure 6C).

Cellular localization and transcriptional function of CVB3-mediated SRF cleavage fragments

To understand the functional significance of CVB3-induced SRF cleavage, we generated two constructs

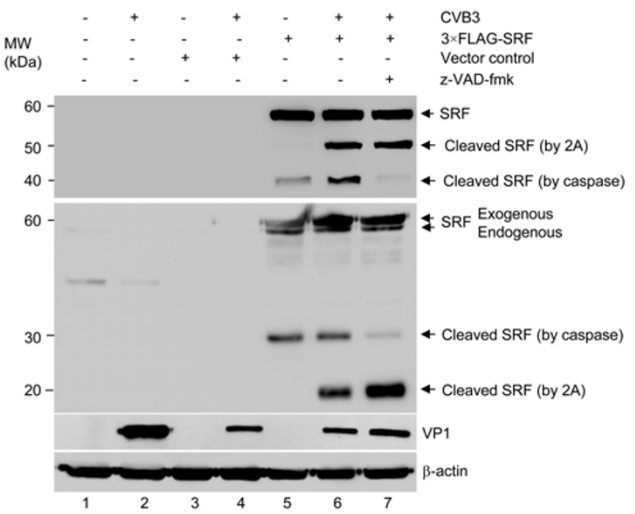

Figure 4 Effect of caspase inhibition on CVB3-induced cleavage of SRF. HeLa cells were transiently transfected with a plasmid expressing 3×FLAG-SRF or an empty vector for 48 h, followed by CVB3 infection for 7 h in the presence or absence of z-VAD-fmk (50 μM), a pan caspase inhibitor. Western blotting was performed to examine protein expression of SRF (top, using anti-FLAG antibody; middle, using anti-C-terminal SRF antibody), viral protein VP1, and β-actin (loading control).

expressing the N- and C-terminal SRF fragments, respectively. We showed that the SRF-N truncate harboring a DNA-binding domain and a nuclear localization signal was localized to the nucleus in both HeLa cells (Figure 7A) and HL-1 cardiomyocytes (Figure 7B) as expected, whereas SRF-C which carries a transcriptional activation domain was distributed in the cytoplasm (Figure 7A) or in both cytosol and nucleus (Figure 7B).

To determine the transcriptional activities of cleaved or non-cleavable SRFs, HeLa cells (Figure 7C) and HL-1 cardiomyocytes (Figure 7D) were transiently co-transfected with Firefly luciferase reporter construct containing cardiac α-actin promoter together with plasmids encoding full-length, truncated, or non-cleavable SRFs and LacZ (control). As displayed in Figure 7C and 7D, the cardiac α-actin promoter activities were strikingly increased with the addition of wild-type and non-cleavable forms of SRF. However, both SRF-N and SRF-C mutants lost their gene transcriptional functions. Our results suggest that CVB3-induced cleavage of SRF leads to the disruption of SRF-mediated gene transactivation.

In addition to loss of function of SRF, the presence of SRF cleavage products may themselves have detrimental effects on the function of native SRF. The N-terminal fragment of SRF contains an intact DNA-binding domain but lacks the C-terminal transactivation domain. To test whether this fragment can act as a dominant-negative competitor to full-length SRF, we co-transfected wild-type SRF together with SRF-N and SRF-C mutants in the presence of cardiac α-actin reporter and Renilla luciferase control plasmids into HeLa cells (Figure 7C) and HL-1 cardiomyocytes (Figure 7D). We demonstrated that the SRF-N mutant significantly decreased wild-type SRF-induced promoter activities of cardiac α-actin, suggesting a negative regulatory role of this mutant in regulating SRF function probably by competing for DNA binding.

Effects of CVB3-mediated SRF cleavage on viral replication

Viruses usually utilize or modulate the host cell infrastructure for their own replication. To test whether cleavage of SRF is beneficial to viral propagation within the host cells, finally, we examined the influences of SRF cleavage on viral replication. Figure 8 showed that neither knockdown of SRF nor overexpression of wild-type or truncated SRFs affects viral replication, suggesting that cleavage of SRF may not contribute directly to viral benefits.

Discussion

Enteroviral proteases have been recognized as an important contributor to viral pathogenesis and resultant myocardial dysfunction via the cleavage of important host proteins. Using a Cre/LoxP-inducible system, it has been shown that transgenic mice with cardiac-specific overexpression of protease 2A develop severe cardiac dysfunction and DCM [3]. Experimental evidence from cell culture and cell-free *in vitro* studies demonstrates that viral protease 2A induces the cleavage and functional impairment of dystrophin [4]. Dystrophin connects the cytoskeletal actin-binding site to the β-dystroglycan extracellular matrix anchor, thus its cleavage leads to the disruption of the cytoskeletal architecture. It is therefore proposed that protease 2A-induced DCM is associated with disrupted myocyte integrity via the cleavage of dystrophin [4]. However, the mdx (dystrophin deficient) mice display a relatively mild dilated phenotype. This is attributed to the compensatory upregulation of the dystrophin homolog utrophin, as evidenced by severe dystrophic phenotype in mice with double knockout of utrophin and dystrophin [5, 6, 27, 28]. Previous study has shown that CVB3 infection does not lead to cleavage of utrophin [4], thus the DCM phenotype induced by dystrophin cleavage may be dampened by the compensatory effect of utrophin in the CVB3-infected heart. All of these suggest that dystrophin cleavage alone may not

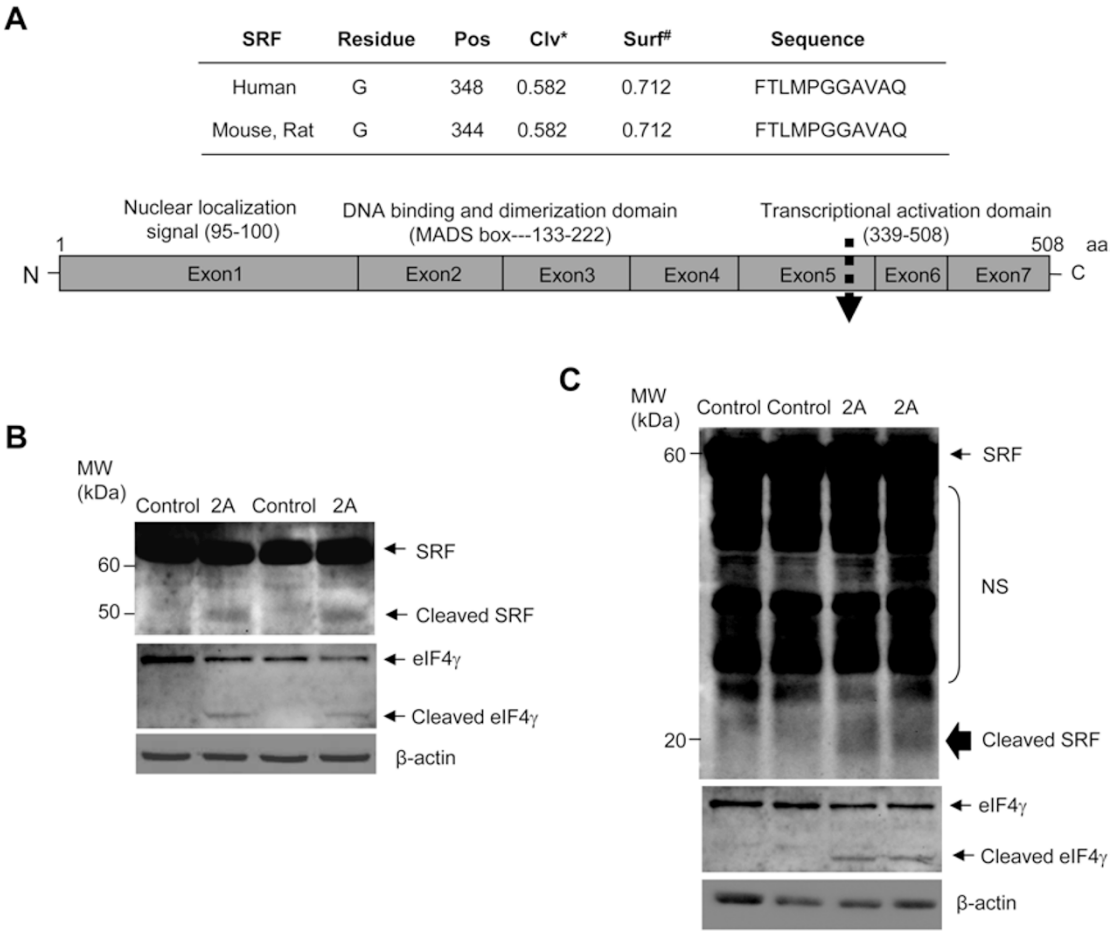

Figure 5 Cleavage of SRF by overexpressing viral protease 2A. **(A)** SRF prediction cleavage site for viral protease 2A. The SRF protein sequence was searched for putative cleavage sites of picornavirus proteases using NetPicoRNA V1.0 algorithm. *Cleavage prediction score above 0.500 are predicted as potential cleavage sites. #Surface exposure scores above 0.500 are predicted as surface exposed sites. **(B**, **C)** HeLa cells were transiently transfected with 3×FLAG-tagged SRF construct for 48 h, followed by additional transfection with either empty vector (control) or viral protease 2A plasmid for another 48 h. Western blotting was performed to examine protein expression of SRF using anti-FLAG antibody **(B)** that recognizes the N-terminus of SRF, or by anti-C-terminal SRF antibody **(C)**. The 2A proteolytic activity was confirmed by the cleavage of eIF4γ. Expression of β-actin was shown as a loading control. NS, nonspecific bands.

be sufficient to explain the severe cardiomyopathy phenotype observed in 2A-transgenic mice. This prompts us to postulate that other substrate(s) of 2A may also play a role in the progression of virus-induced cardiomyopathy.

The major findings of this study are as follows: (1) cardiac-specific contractile and regulatory genes are downregulated in CVB3-infected mouse heart and cardiomyocytes, (2) SRF is cleaved by viral protease 2A during CVB3 infection, and (3) cleavage of SRF leads to the disruption of SRF-mediated gene transactivation and production of a dominant-negative competitor to native SRF. These findings suggest that SRF cleavage may contribute to cardiac dysfunction and subsequent progression to DCM in enteroviral myocarditis by disturbing the expression of cardiac contractile and regulatory genes.

Microarray studies in human end-stage heart failure revealed a significant downregulation of numerous cardiac genes, including genes with SRF-binding sites, implicating an important role of SRF in the progression of heart failure [22-24]. In the present study, we provide the first evidence that cardiac-specific genes are also downregulated in enterovirus-infected heart and cultured cardiomyocytes. All these genes shown in Figure 1 have either been previously reported to be targets of SRF or contain SREs in their promoter regions [10, 29, 30].

It was reported that expression of an alternatively spliced SRF variant lacking portions of the transactivation domain is markedly increased in human and animal

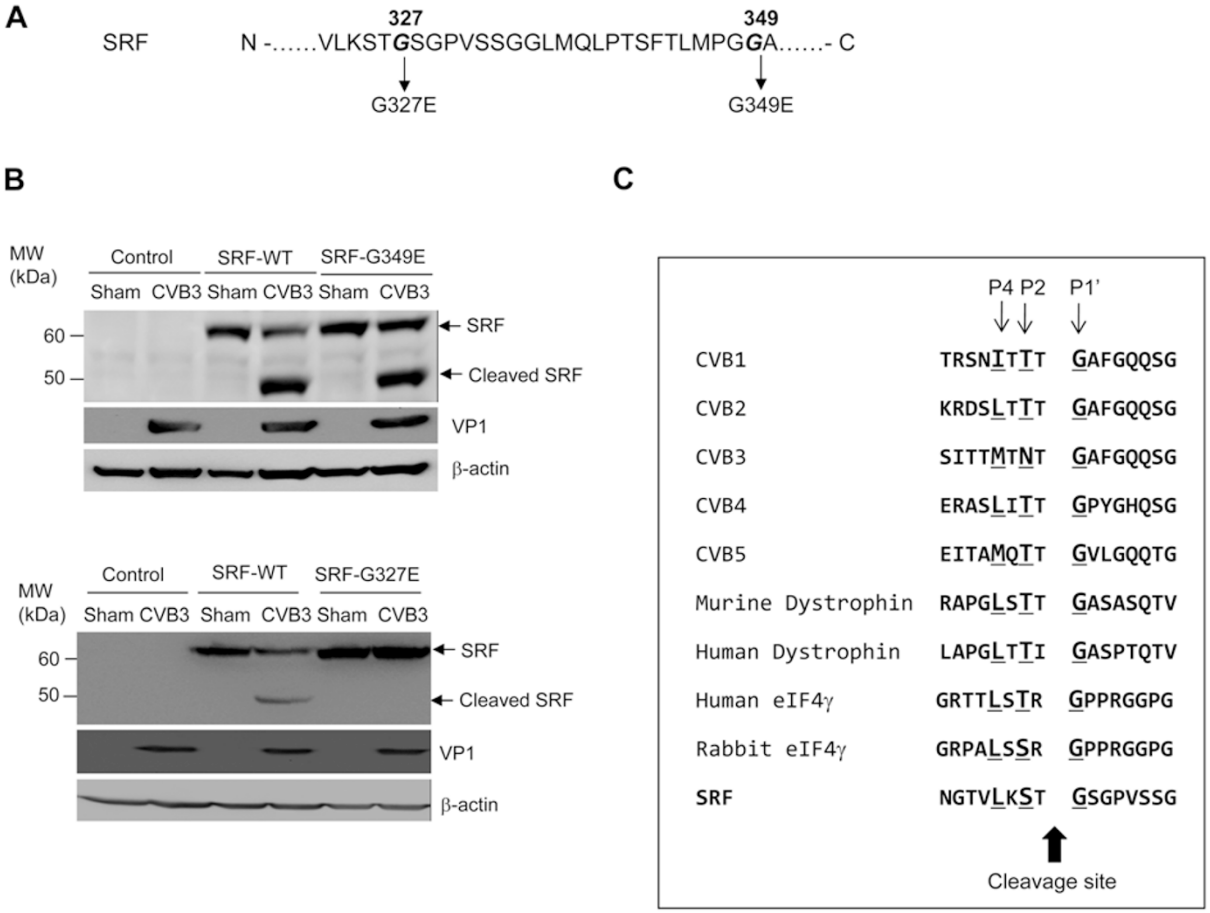

Figure 6 Cleavage of SRF after T326 following CVB3 infection. **(A)** Diagram of point mutation constructs of SRF. **(B)** HeLa cells were transiently transfected with 3×FLAG-tagged SRF-wild-type (SRF-WT) or SRF mutants (SRF-G349E or SRF-G327E as indicated) for 48 h, followed by 7 h CVB3 infection. Transfection of an empty vector (pcDNA) was used as negative controls. Western blotting was performed to examine protein expression of SRF using anti-FLAG antibody and viral protein VP1. Expression of β-actin was shown as a loading control. NS, nonspecific bands. **(C)** Identification of protease 2A substrate cleavage site. Substrate recognition by 2A depends on a degenerate amino acid pattern upstream of the cleavage site. The cleavage recognition site usually contains a T, or S at position P2 and an L, I, or M at position P4. A glycine residue at the P1′ C-terminal side of the scissile bond of the cleavage site occurs in all known substrates of the 2A protease.

failing hearts [31, 32]. This isoform functions as a dominant-negative mutant that inhibits SRF-dependent activation of cardiac muscle genes. Interestingly, our recent report showed that SRF cleavage also occurs in myocytes of severely failing human hearts. Increased caspase activity during heart failure induces the cleavage of SRF, producing a truncated protein that lacks the C-terminal transactivation domain, and acts as a dominant inhibitory transcription factor, similar to the alternatively spliced variant [19]. These studies suggest that decreased production of full-length SRF, or increased accumulation of truncated SRF, may downregulate SRF-dependent genes and contribute to the progression of severe heart failure. In this study, we have identified a new cleavage site in SRF by viral protease 2A during virus infection and demonstrated a dominant-negative effect of the cleaved SRF on the expression of cardiac genes.

Coxsackievirus infection of heart results in focal lesions accompanied by severe fibrosis. Interestingly, recent research on mosaic regional inactivation of SRF in mouse hearts was found to be sufficient in inducing focal lesions and resulting in fatal DCM [33]. In these mice, wild-type cardiomyocytes adjacent to the SRF-null myocytes undergo compensatory hypertrophy, which further triggers a hypertrophic response in remote wild-type cardiomyocytes to preserve cardiac output. This mosaic SRF inactivation model provides some insights into the possible pathophysiological consequences of non-

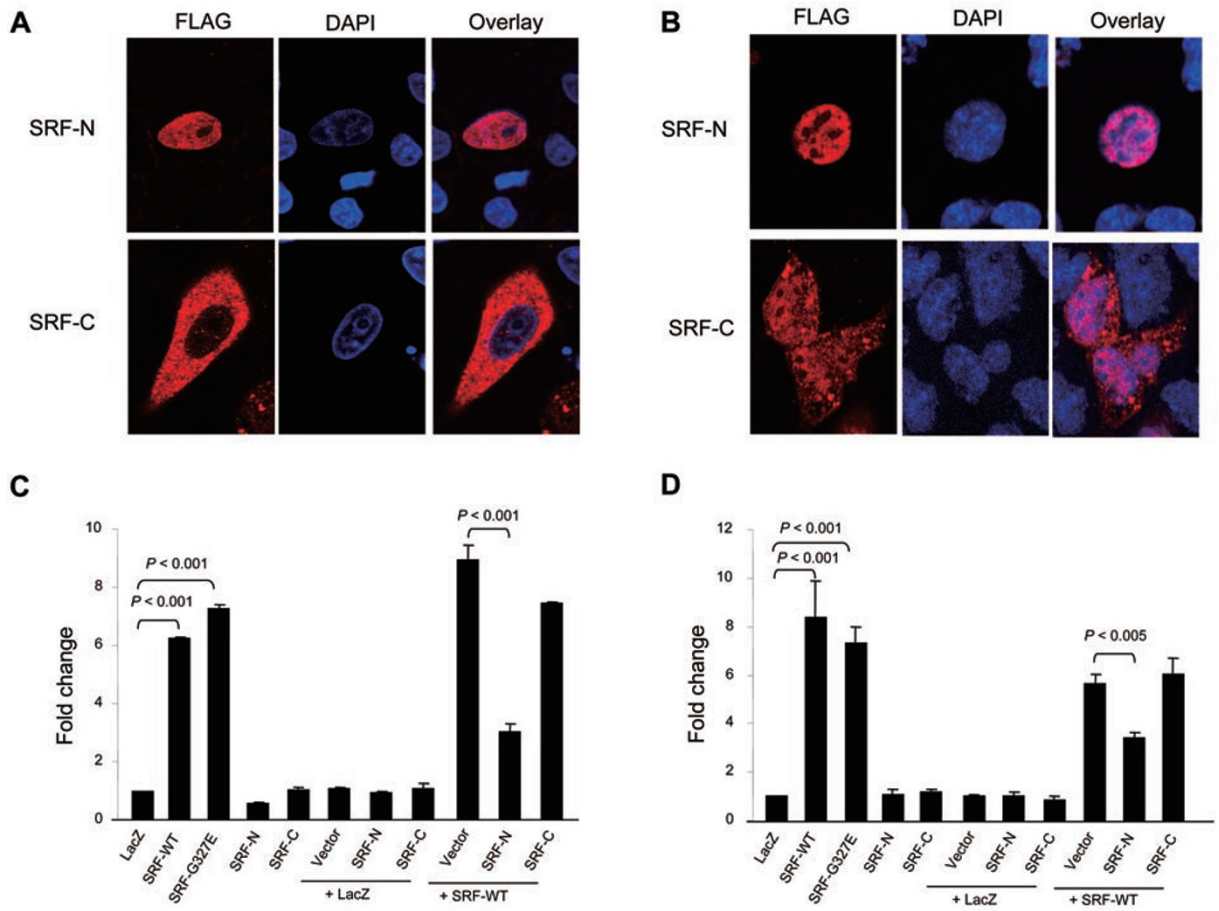

Figure 7 Cellular localization and transcriptional activity of SRF mutants. **(A**, **B)** HeLa cells **(A)** or HL-1 cardiomyocytes **(B)** were transiently transfected with 3×FLAG-tagged SRF-N or SRF-C fragments of the cleaved SRF products for 48 h using Lipofectamine 2000. Immunocytochemical staining for transfected SRF was performed using anti-FLAG antibody. Nucleus was counterstained with DAPI. **(C**, **D)** HeLa cells **(C)** or HL-1 cardiomyocytes **(D)** were transiently co-transfected with cardiac α-actin luciferase reporter plasmid and constructs expressing SRF-WT or empty vector and/or SRF-G327E, SRF-N, and SRF-C mutants as indicated for 48 h. Luciferase assay was performed and the values are presented as folder changes (mean ± SD, *n* = 3) over those of control reporter (LacZ), which were arbitrarily set as 1.

functional SRF and dominant-negative SRF truncates presented in patches of CVB3-infected cardiomyocytes and their subsequent influences on the disease progression and outcome.

Overexpression of SRF has also been associated with cardiac hypertrophy. Transgenic mouse studies showed that the cardiac-specific overexpression of SRF induces a pattern of fetal gene re-expression similar to that observed in cardiac hypertrophy and subsequently causes a severe hypertrophic phenotype [34]. Therefore, in the future, establishment of a knockin mouse model expressing non-cleavable SRF in the heart will be crucial to determine whether this form of SRF can rescue cardiomyocytes from CVB3-induced dysfunction.

In conclusion, our results provide new insights into the mechanisms by which virus infection impairs heart function and may further the development of new therapeutic approaches to ameliorating myocardial damage and progression to DCM.

Materials and Methods

Cell culture and in vitro CVB3 infection

The HL-1 cell line, a murine cardiac muscle cell line established from an AT-1 mouse atrial cardiomyocyte tumor lineage, was a generous gift from Dr William C Claycomb (Louisiana State University Medical Center, USA). Cells were plated and maintained in Claycomb medium (JRH Biosciences) supplemented with 10% fetal bovine serum, 100 μg/ml penicillin-streptomycin, 0.1 mM norepinephrine in ascorbic acid, and 2 mM L-glutamine as described previously [35]. HL-1 cardiomyocytes were infected

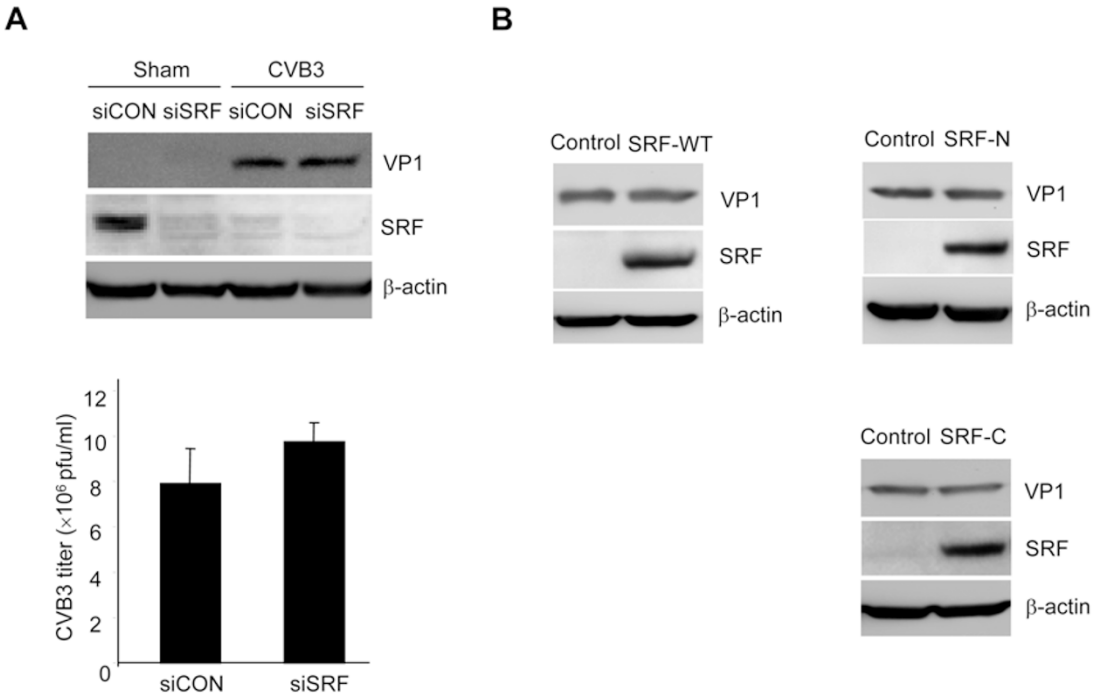

Figure 8 Effects of SRF dysregulation on CVB3 replication. **(A)** Effects of knockdown of SRF on CVB3 replication. The gene expression of SRF was knocked down by siRNA. siCON, scramble siRNA control. Upper, western blot analysis was carried out to examine protein level of viral protein VP1, SRF (with anti-FLAG antibody), and β-actin (loading control). Lower, plaque assay was performed to examine virus titers. The results are shown as mean ± SD (n = 3). **(B)** Effect of overexpression of SRF-wild-type (SRF-WT) and two truncated SRF mutants on CVB3 replication. HeLa cells were transiently transfected with SRF-WT or truncated SRF mutants (SRF-N or SRF-C as indicated) for 48 h, followed by 7 h CVB3 infection. Western blot analysis was carried out to examine protein level of viral protein VP1, SRF (with anti-FLAG antibody) and β-actin (loading control).

at a multiplicity of infection (MOI) of 10 with CVB3 (Kandolf strain) or sham infected with phosphate-buffered saline (PBS) for 1 h, washed with PBS, and placed in complete culture medium for various times.

HeLa cells were obtained from the American Type Culture Collection. Cells were grown in Dulbecco's modified Eagle's medium (DMEM) supplemented with 10% heat-inactivated newborn calf serum. HeLa cells were infected in a similar fashion as described above.

In vivo CVB3 infection and heart functional measurements

Male A/J mice at the age of ~5 weeks were either infected intraperitoneally with 10^5 plaque-forming unit (p.f.u.) of CVB3 or sham infected with PBS for 3, 9, and 30 days. Heart function was measured before infection (day 0) and on days 3, 9, and 30 after CVB3 infection using two-dimensional echocardiography (Sonos 5500, Philips) with a 12 MHz S-12 probe (Sonos 5000). Parasternal long and short axis images at the level of the mitral valve and papillary muscles were taken and these measurements were normalized to changes in body weight and then utilized for calculation of functional parameters. All measurements were averaged for five consecutive cardiac cycles.

This study was carried out in strict accordance with the recommendations in the Guide for the Care and Use of Laboratory Animals of the Canadian Council on Animal Care. The protocol was approved by the Animal Care Committee of the University of British Columbia (#A03-0233).

Affymetrix array analysis

Hearts were harvested at 9 days following CVB3 infection and total RNA was isolated from mouse ventricular tissue using the RNeasy® isolation kit (Qiagen) and pooled (n = 4 for each group). Samples were hybridized to a custom mouse GeneChip® (Amgen) based on the Affymetrix GeneChip® Expression Analysis Technical Manual (Affymetrix). *In vitro* transcription was performed using an ENZO Bioarray™ HighYield™ RNA Transcript Labeling kit as per the manufacturer's instructions. Arrays were washed in the Affymetrix Fluidics Station 450, stained with a streptavidin phycoerythrin solution and scanned using a HP Agilent GeneArray® Scanner.

Western blot analysis

Protein concentrations of cell or tissue lysates were determined by the Bradford assay (Bio-Rad Laboratories). Equal amounts of protein were subjected to SDS-PAGE and then transferred to a nitrocellulose membrane. The membrane was blocked with 5% non-fat dry milk solution containing 0.1% Tween-20 for 1 h. Afterwards, the membrane was probed for 1 h with the primary anti-

body, followed by incubation for 1 h with horseradish peroxidase-conjugated secondary antibody. Immunoreactive bands were visualized with enhanced chemiluminescence (SuperSignal).

The following antibodies were utilized: monoclonal anti-β-actin and anti-GAPDH (Sigma), monoclonal anti-VP1 (DakoCytomation), polyclonal anti-SRF N-terminus (Novus Biological), polyclonal anti-SRF C-terminus, anti-FLAG, and anti-eIF4γ (Santa Cruz Biotechnology).

Immunocytochemistry

Cells grown on glass slides were washed with PBS and fixed in 4% formaldehyde. Cells were then permeabilized with 0.1% Triton X-100 for 10 min, blocked with 5% bovine serum albumin (BSA) in Tris-buffered saline (TBS) for 30 min. After incubation with primary antibodies at 4 °C overnight and then with anti-rabbit AlexaFluor 594 or anti-mouse AlexaFluor 488 IgG at room temperature for 1 h, cells were washed with PBS and then mounted on slides using VectaShield medium containing 4′,6-diamidino-2-phenylindole (DAPI). Cells were imaged and analyzed using a Leica SP2 AOBS confocal fluorescence microscope.

Real-time quantitative RT-PCR

Total RNAs were extracted from murine HL-1 cardiomyocytes at 24 h post infection. Following reverse transcription, the mRNA levels of SRF and cardiac genes were measured by real-time quantitative PCR using an ABI Prism 7900HT Sequence Detection System as per the manufacturers' instruction (Perkin-Elmer Applied Biosystems) as previously described [20] and normalized to GAPDH mRNA.

Constructs

The pCMV-3×FLAG-SRF construct, a generous gift from Dr Ron Prywes (Columbia University, USA), was used as the template for the generation of site-directed mutagenesis (SRFG349E and SRFG327E mutants). Truncated SRF cDNAs were generated by PCR using the following primers: SRF-N forward 5′-GTCGACTCTAGAATGTTACCG-3′ and reverse 5′-AGGAGACGGATCCGCTTCATG-3′; SRF-C forward 5′-CTGAAGTCTAGAGGCAGCGG-3′ and reverse 5′-ACCCGGGATCCTTTAGATCAT-3′. SRF-N and SRF-C cDNAs were subcloned into pCMV-3×FLAG vector using *Xba*I and *Bam*HI restriction digestions.

Luciferase assay

HeLa and HL-1 cells at 90% confluence in 24-well tissue culture plates were transiently co-transfected with a Firefly luciferase reporter construct containing cardiac α-actin promoter [19] and a Renilla luciferase control vector (Promega) together with plasmids encoding full-length, truncated, or non-cleavable SRFs, and control LacZ. After 48 h, cell lysates were collected and analyzed for firefly and renilla luciferase activities using a dual luciferase reporter assay system (Promega) as per the manufacturer's instruction. The relative luciferase activities were normalized to the LacZ control group and presented as fold changes.

Plaque assay

Virus titer in cell supernatant was measured by an agar overlay plaque assay. In brief, cell supernatant was serially diluted and overlaid on a 90% to 95% confluent monolayer of HeLa cells. After 1 h of incubation, cells were washed with PBS and overlaid with complete DMEM containing 0.75% agar. At 3 days after infection, cells were fixed with Carnoy's fixative (75% ethanol and 25% acetic acid) and stained with 1% crystal violet. Plaques were counted, and the viral titer was determined as p.f.u./ml.

Small-interfering RNA (siRNA)

HeLa cells grown at 50% confluence were transfected with SRF or control siRNAs (Santa Cruz Biotechnology) using Lipofectamine 2000. After 48 h, cells were infected with CVB3 as described above. Cell supernatants and lysates were collected 7 h post infection and analyzed for viral titer and protein expression by plaque assay and western blotting, respectively.

Statistical analysis

Results are expressed as mean ± SD. Statistical analysis was performed with unpaired Student's *t*-test. *P*-values < 0.05 were considered to be statistically significant.

Acknowledgments

This work was supported by the Heart and Stroke Foundation of British Columbia and Yukon (to HL), the Canadian Institutes of Health Research (to HL), the American Heart Association (0855030F to JC) and the American National Institutes of Health (R01HL102314, R21HL094844 and K0202HL098956 to JC). JW was awarded the Studentship from the Canadian Institutes of Health Research.

References

1 Luo H, Wong J, Wong B. Protein degradation systems in viral myocarditis leading to dilated cardiomyopathy. *Cardiovasc Res* 2010; **85**:347-356.
2 Yajima T, Knowlton KU. Viral myocarditis: from the perspective of the virus. *Circulation* 2009; **119**:2615-2624.
3 Xiong D, Yajima T, Lim BK, *et al.* Inducible cardiac-restricted expression of enteroviral protease 2A is sufficient to induce dilated cardiomyopathy. *Circulation* 2007; **115**:94-102.
4 Badorff C, Lee GH, Lamphear BJ, *et al.* Enteroviral protease 2A cleaves dystrophin: evidence of cytoskeletal disruption in an acquired cardiomyopathy. *Nat Med* 1999; **5**:320-326.
5 Deconinck AE, Rafael JA, Skinner JA, *et al*. Utrophin-dystrophin-deficient mice as a model for Duchenne muscular dystrophy. *Cell* 1997; **90**:717-727.
6 Grady RM, Teng H, Nichol MC, *et al.* Skeletal and cardiac myopathies in mice lacking utrophin and dystrophin: a model for Duchenne muscular dystrophy. *Cell* 1997; **90**:729-738.
7 Miano JM. Serum response factor: toggling between disparate programs of gene expression. *J Mol Cell Cardiol* 2003; **35**:577-593.
8 Niu Z, Li A, Zhang SX, Schwartz RJ. Serum response factor micromanaging cardiogenesis. *Curr Opin Cell Biol* 2007; **19**:618-627.
9 Oka T, Xu J, Molkentin JD. Re-employment of developmental transcription factors in adult heart disease. *Semin Cell Dev Biol* 2007; **18**:117-131.
10 Sun Q, Chen G, Streb JW, *et al.* Defining the mammalian CArGome. *Genome Res* 2006; **16**:197-207.

11 Liu N, Bezprozvannaya S, Williams AH, *et al.* MicroRNA-133a regulates cardiomyocyte proliferation and suppresses smooth muscle gene expression in the heart. *Genes Dev* 2008; **22**:3242-3254.
12 Miano JM, Ramanan N, Georger MA, *et al.* Restricted inactivation of serum response factor to the cardiovascular system. *Proc Natl Acad Sci USA* 2004; **101**:17132-17137.
13 Nelson TJ, Balza R Jr, Xiao Q, Misra RP. SRF-dependent gene expression in isolated cardiomyocytes: regulation of genes involved in cardiac hypertrophy. *J Mol Cell Cardiol* 2005; **39**:479-489.
14 Niu Z, Iyer D, Conway SJ, *et al.* Serum response factor orchestrates nascent sarcomerogenesis and silences the biomineralization gene program in the heart. *Proc Natl Acad Sci USA* 2008; **105**:17824-17829.
15 Small EM, O'Rourke JR, Moresi V, *et al.* Regulation of PI3-kinase/Akt signaling by muscle-enriched microRNA-486. *Proc Natl Acad Sci USA* 2010; **107**:4218-4223.
16 Zhao Y, Ransom JF, Li A, *et al.* Dysregulation of cardiogenesis, cardiac conduction, and cell cycle in mice lacking miRNA-1-2. *Cell* 2007; **129**:303-317.
17 Parlakian A, Tuil D, Hamard G, *et al.* Targeted inactivation of serum response factor in the developing heart results in myocardial defects and embryonic lethality. *Mol Cell Biol* 2004; **24**:5281-5289.
18 Parlakian A, Charvet C, Escoubet B, *et al*. Temporally controlled onset of dilated cardiomyopathy through disruption of the SRF gene in adult heart. *Circulation* 2005; **112**:2930-2939.
19 Chang J, Wei L, Otani T, *et al.* Inhibitory cardiac transcription factor, SRF-N, is generated by caspase 3 cleavage in human heart failure and attenuated by ventricular unloading. *Circulation* 2003; **108**:407-413.
20 Cheung C, Marchant D, Walker EK, *et al.* Ablation of matrix metalloproteinase-9 increases severity of viral myocarditis in mice. *Circulation* 2008; **117**:1574-1582.
21 Marchant D, Dou Y, Luo H, *et al.* Bosentan enhances viral load via endothelin-1 receptor type-A-mediated p38 mitogen-activated protein kinase activation while improving cardiac function during coxsackievirus-induced myocarditis. *Circ Res* 2009; **104**:813-821.
22 Barrans JD, Allen PD, Stamatiou D, Dzau VJ, Liew CC. Global gene expression profiling of end-stage dilated cardiomyopathy using a human cardiovascular-based cDNA microarray. *Am J Pathol* 2002; **160**:2035-2043.
23 Hwang JJ, Allen PD, Tseng GC, *et al.* Microarray gene expression profiles in dilated and hypertrophic cardiomyopathic end-stage heart failure. *Physiol Genomics* 2002; **10**:31-44.
24 Tan FL, Moravec CS, Li J, *et al.* The gene expression fingerprint of human heart failure. *Proc Natl Acad Sci USA* 2002; **99**:11387-11392.
25 Bertolotto C, Ricci JE, Luciano F, *et al.* Cleavage of the serum response factor during death receptor-induced apoptosis results in an inhibition of the c-FOS promoter transcriptional activity. *J Biol Chem* 2000; **275**:12941-12947.
26 Drewett V, Devitt A, Saxton J, *et al.* Serum response factor cleavage by caspases 3 and 7 linked to apoptosis in human BJAB cells. *J Biol Chem* 2001; **276**:33444-33451.
27 Hainsey TA, Senapati S, Kuhn DE, Rafael JA. Cardiomyopathic features associated with muscular dystrophy are independent of dystrophin absence in cardiovasculature. *Neuromuscul Disord* 2003; **13**:294-302.
28 Janssen PM, Hiranandani N, Mays TA, Rafael-Fortney JA. Utrophin deficiency worsens cardiac contractile dysfunction present in dystrophin-deficient mdx mice. *Am J Physiol Heart Circ Physiol* 2005; **289**:H2373-2378.
29 Balza RO Jr, Misra RP. Role of the serum response factor in regulating contractile apparatus gene expression and sarcomeric integrity in cardiomyocytes. *J Biol Chem* 2006; **281**:6498-6510.
30 Chai J, Tarnawski AS. Serum response factor: discovery, biochemistry, biological roles and implications for tissue injury healing. *J Physiol Pharmacol* 2002; **53**:147-157.
31 Belaguli NS, Zhou W, Trinh TH, Majesky MW, Schwartz RJ. Dominant negative murine serum response factor: alternative splicing within the activation domain inhibits transactivation of serum response factor binding targets. *Mol Cell Biol* 1999; **19**:4582-4591.
32 Davis FJ, Gupta M, Pogwizd SM, *et al.* Increased expression of alternatively spliced dominant-negative isoform of SRF in human failing hearts. *Am J Physiol Heart Circ Physiol* 2002; **282**:H1521-H1533.
33 Gary-Bobo G, Parlakian A, Escoubet B, *et al.* Mosaic inactivation of the serum response factor gene in the myocardium induces focal lesions and heart failure. *Eur J Heart Fail* 2008; **10**:635-645.
34 Zhang X, Azhar G, Chai J, *et al.* Cardiomyopathy in transgenic mice with cardiac-specific overexpression of serum response factor. *Am J Physiol Heart Circ Physiol* 2001; **280**:H1782-H1792.
35 Luo H, Zhang J, Cheung C, *et al.* Proteasome inhibition reduces coxsackievirus B3 replication in murine cardiomyocytes. *Am J Pathol* 2003; **163**:381-385.

(**Supplementary information** is linked to the online version of the paper on the *Cell Research* website.)